

From Lithospheric Thickening and Divergent Collapse to
Active Continental Rifting

Patrice F. Rey

School of Geosciences, University of Sydney

NSW2006 Sydney, Australia

Published in Miller, J.A., Buick, I.S., Hand, M., and Holdsworth, R.E., (eds),

Continental Reworking and Reactivation,

Journal of the Geological Society of London, v.184

July 22, 2006

Contents

1	Abstract	3
2	Introduction	3
3	Modelling Approach, Main Assumptions and Simplifications	5
3.1	Tectonic thickening	6
3.2	Erosion/Sedimentation	6
3.3	Thermal relaxation	7
3.4	Gravity-driven flow	7
4	Physical Model	7
4.1	Temperature profile	8
4.2	Density profile and surface elevation	8
4.3	Gravitational force	9
4.4	Strength profile	10
4.5	Lithospheric geometry through time	10
5	Presentation of the results	11
5.1	Stable Thermal Boundary Layer during convergence	11
5.2	Post-convergence removal of the Thermal Boundary Layer	12
6	Discussion and conclusion	13
7	Acknowledgements	15
8	References	16

1 Abstract

The Aegean Sea, the Alboran Sea, and the Basin and Range Province suggest that continental lithosphere following gravitational collapse may end up being thinner than it was before convergence and thickening. In order to assess the condition leading to the development of finite lithosphere thinning following convergence and convective thinning, the strength of the continental lithosphere, the gravitational force, and the rate of gravity-driven flow (spreading rate) are calculated during and after continental collision. One dimensional numerical experiments, presented here, assume that the deformation is homogeneous, that erosion is a function of strain rate and elevation and that thermal relaxation involves no lateral conduction of heat. Results show that if 43% of the lower lithospheric mantle is dragged into the convective mantle (convective thinning), gravitational collapse may lead to a lithosphere thinner than the initial lithosphere (pre-thickening lithosphere), provided that gravitational collapse is accommodated by the passive displacement of the surrounding lithosphere (free boundary collapse). When a slightly larger volume of lithospheric mantle is removed, a phase of extension leading to a necking instability and the formation of an active rift follows collapse. The presence of fixed boundaries and/or horizontal compressive stresses strongly reduces the spreading rate and opposes finite lithosphere thinning and therefore active rifting. It is suggested that back-arc extension occurring in continental settings could exemplify post-collapse active rifting.

2 Introduction

Thermal thinning of the lithospheric mantle (above a mantle plume for instance) has been proposed as the driving mechanism for active continental rifting (Le Pichon, 1983; Turcotte and Emerman, 1983; Le Pichon and Alvarez, 1984). Although normal stresses imposed at the base of the lithosphere by the plume may be important (Houseman and Thermal thinning of the lithospheric mantle (above a mantle plume for instance) has been proposed as the driving mechanism for active continental rifting (Le Pichon, 1983; Turcotte and Emerman, 1983; Le Pichon and Alvarez, 1984). Although normal stresses imposed at the base of the lithosphere by the plume may be important (Houseman and England, 1986), active continental rifting is usually related to gravity-related tensile stresses induced by thinning of the lithospheric mantle. Alternatively, thinning of the lithospheric mantle can

be achieved through convective thinning following lithospheric thickening (Houseman et al., 1981). This process increases the gravitational potential energy of the thickened lithosphere producing tensile horizontal stresses that may trigger divergent collapse: The gravity-driven flow that reduces lateral variation of gravitational potential energy. As collapse proceeds, the thickened crust tends to recover its normal thickness and, assuming homogeneous deformation, the lithospheric mantle becomes thinner than it was before convergence and thickening. Therefore, the rise of a mantle plume underneath a lithosphere of normal thickness and divergent collapse following thickening and convective thinning may result in similar vertical lithospheric geometry where a continental crust of normal thickness overlies a thin lithospheric mantle (Fig. 1). Tensile horizontal stresses that arise from this geometry may be strong enough to induce self-enhanced lithospheric thinning. Should the extensional strain rates be too slow, this thinning will be limited by thermal relaxation and cooling, leading to aborted rifts. Should convergence occur in the next couple of hundred Ma, this thinned lithosphere will, most likely, localise contractional deformation. In contrast, a fast extensional strain rates could lead to active continental rifting and the formation of continental margins. In both cases orogenic collapse could explain why orogenic belts tend to be the sites of successive orogenesis. Much has been written about gravitational collapse (e.g., England and McKenzie, 1982; Molnar and Chen, 1982, 1983; Coney and Harms, 1984; Dewey, 1988; England and Houseman, 1988, 1989; Molnar and Lyon-Caen, 1988; Rey et al., 2001), and its thermal and mechanical consequences (e.g., Platt and England, 1993; Rey, 1993; Mareschal, 1994; Costa and Rey, 1995). One aspect that still needs to be addressed is how collapsed orogenic lithospheres such as in the Basin and Range, the Aegean Sea, the Alboran Sea, and the Carpathian Basin, end up being thinner than they were before thickening. Through simple 1D numerical experiments, this paper explores the evolution of the spreading strain rate as the key parameter for mapping the evolution of both integrated lithospheric strength and gravitational force driving extension. Some of the experiments suggest that, should convective thinning occur, the crust and the lithosphere will end up being significantly thinner and weaker for at least a few hundreds of Ma, and therefore prone to tectonic reactivation. In some favourable cases, some experiments show that collapse could even be followed by self-enhanced extension leading to a necking instability and the formation of a continental rift.

3 Modelling Approach, Main Assumptions and Simplifications

Numerical experiments on simplified lithosphere systems provide quantitative insights into orogenic processes, and allow investigation of the consequences of some theoretical processes. The numerical design involves building a simplified lithosphere whose vertical geometry changes under the action of four processes: (i) plane strain homogeneous deformation driven convergence, (ii) erosion/sedimentation, (iii) thermal relaxation, and (iv) gravitational spreading. In order to maintain isostatic equilibrium, these four processes are implemented successively over small increments of time, a Crank-Nicholson finite differences scheme being used for the treatment of the thermal relaxation. In conjunction, a thin sheet approximation is used which considers stresses and strain rates in terms of their vertical average through the lithosphere (e.g., England and Houseman, 1988, 1989). Given knowledge of the rheology of the continental lithosphere, and knowing the gravitational force acting on the deformed lithosphere, one can calculate the strain rate of the gravity-related flow and that of the convergence-related flow. It is assumed for simplicity that both flows occur in two perpendicular directions. The evolution of the geometry of the lithosphere can be portrayed as a path within the $f_c - f_l$ plane (Fig. 2) where f_c is the thickness ratio of the thickened crust to that of the reference crust (z_c), and f_l is the thickness ratio of the thickened lithosphere to that of the reference lithosphere (z_l) (Sandiford and Powell, 1990). During deformation the deforming lithosphere follows a path in the $f_c - f_l$ plane which starts at $f_c = f_l = 1$ (ie. an undeformed reference state). Convergent orogens attain higher f_c and f_l values, while thinned lithosphere evolves to f_c and f_l values ≤ 1 (Fig. 2). The triangular field at high f_c and low f_l values portrays the condition where the lithosphere consists entirely of crust (ie. where $f_c \cdot z_c \leq f_l \cdot z_l$). This paper employs a slight variation in the representation of the $f_c - f_l$ plane to that originally defined by Sandiford and Powell (1990). The $f_c - f_l$ plane is here oriented so that the crustal component of the lithosphere is lying above the mantle component. In this orientation the $f_c - f_l$ plane becomes more illustrative, with the column above any point of the $f_c - f_l$ plane representing a lithospheric column with its mantle and crustal component. What follows describes the main assumptions related to the four processes that affect the vertical geometry of the continental lithosphere.

3.1 Tectonic thickening

A reference lithosphere ($z_c=35$ km, $z_l=104$ km), in isostatic and mechanical equilibrium with a column beneath the mid-ocean ridge, is submitted to a tectonic force (F_d) to achieve a constant strain rate of 10^{-15} s $^{-1}$. As the lithosphere becomes thicker and stronger, F_d must increase to maintain a constant strain rate. It is assumed here that the maximum magnitude for F_d is 30×10^{12} Nm $^{-1}$ (e.g. Bott, 1993). When this value is reached the strain rate decreases as thickening proceeds. When the strain rate is no longer of significance, one can expect thickening to be partitioned into adjacent portions of the orogen leading to the development of a plateau. In the $f_c - f_l$ plane, homogenous deformation is represented by a vector parallel to the line that joins the origin of the $f_c - f_l$ plane ($f_c = f_l=0$, top left corner of the $f_c - f_l$ plane) to the point representing the deforming lithosphere. This vector is directed away from the origin in the case of homogeneous thickening, and towards it during homogeneous thinning.

3.2 Erosion/Sedimentation

Erosion is mainly dependent on the wavelength of the topography (sharp relief implying fast erosion rate), and its magnitude (Ruxton and McDougall, 1967; Ahnert, 1970). Most estimations of erosional rates fall in the range of 0.2 to 1mm per year (Clark and Jaeger, 1969; England and Richardson, 1977; Pinet and Souriau, 1988; Mercier et al., 1991). The rate of erosion is assumed here to be proportional to (i) the strain rate (fast strain rates produce sharp relief), and (ii) the difference in elevation between that of the reference lithosphere (+874 m) and that of the deformed lithosphere. This is consistent with the observation that orogenic plateaux are characterised by a relatively flat topography, a slow strain rate, and little erosion. If, at some stage the surface of the lithosphere drops below sea level, it is assumed that sedimentation maintains a constant water/sediment ratio of 2:1 in the basin. In the $f_c - f_l$ plane, erosion/sedimentation is represented by a vector parallel to the boundary between the crust and the mantle (Moho line in Fig. 2) since these processes do not affect the thickness of the sub-continental mantle lithosphere. During erosion, the vector is directed towards the origin of the $f_c - f_l$ plane (the crust becomes thinner and therefore f_c decreases). During sedimentation it is directed away from the origin of the $f_c - f_l$ plane.

3.3 Thermal relaxation

During lithospheric thickening, isotherms are displaced vertically producing a thermal anomaly. Assuming that a constant heat flow is maintained at the base of the lithosphere, defined by the isotherm 1330°C, the relaxation of this thermal anomaly tends to reduce the thickness of the lithospheric mantle. This thermal thinning increases the surface elevation and therefore the tensile gravitational force. During and following thickening, thermal relaxation also tends to increase the average temperature of the lithosphere and therefore tends to reduce its strength. In the $f_c - f_1$ plane, the vector representing thermal relaxation is parallel to the f_1 axis, since this process does not affect the thickness of the crust. The vector is oriented towards higher f_1 values when thermal relaxation increases the thickness of the lithosphere (following thinning), and in the opposite direction when it decreases the thickness of the lithospheric mantle (following thickening).

3.4 Gravity-driven flow

Having assumed that the lithosphere behaves as a viscous thin sheet, the gravitational flow affects the crust and the lithospheric mantle in the same way. The homogeneous gravity-driven flow is represented in the $f_c - f_1$ plane by a vector parallel to the line that joins the origin of the $f_c - f_1$ plane and the point representing the deforming lithosphere. This vector is directed away from the origin of the $f_c - f_1$ plane in the case of convergent gravitational flow (thickening is enhanced by convergent flow), and towards it in the case of divergent flow. Divergent gravitational spreading can be accommodated by either the thickening of the surrounding lithosphere (fixed boundary collapse) or by its passive displacement (free boundary collapse, Rey et al., 2001). Depending on the accommodation mechanism, it is assumed that the spreading rate is buffered by either the shortening rate of the surrounding lithosphere, or the extensional rate of the collapsing lithosphere.

4 Physical Model

What follows describes the parameters that enter in the definition of the balance of forces, and how these parameters change during deformation. To facilitate comparisons with studies that have investigated force balance in convergent orogen, the numerical experiments presented in this paper

use similar physical parameters, simplifications and approximations (Le Pichon and Alvarez, 1984; Sandiford and Powell, 1991; Ranalli, 1992; Zhou and Sandiford, 1992). Table 1 gives a list of symbols, values and parameters used in this paper.

4.1 Temperature profile

The density and strength profile, as well as the gravitational force are dependent on temperature. Steady state and transient geotherms are derived from the one-dimensional diffusion-advection equation:

$$\frac{\delta T}{\delta t} = \frac{\kappa \cdot \delta^2 T}{\delta z^2} + \frac{A}{\rho \cdot C_p} - v \cdot \frac{\delta T}{\delta z} \quad (1)$$

with κ : thermal diffusivity, A : the radiogenic heat production, ρ : the density, C_p : the heat capacity, and v : the velocity. Boundary conditions involve a constant heat flow entering the base of the lithosphere, and a constant temperature at the surface. The velocity of the medium relative to its surface is a function of deformation, erosion/sedimentation, and gravity-driven flow. It was implemented iteratively over small time intervals.

4.2 Density profile and surface elevation

The density profile enters in the calculation of the surface elevation (h) of the lithosphere, which in turn is necessary for calculation of the gravitational force. For the crust a linear density profile is used. It increases from the top of the crust (ρ_a) to the Moho (ρ_b), and is dependent on temperature (β_m the coefficient of thermal expansion).

$$\rho_{\text{crust}}(z) = \rho_a + \frac{\rho_b - \rho_a}{f_c \cdot z_c} \cdot (1 - \alpha_m \cdot T(z)) \quad (2)$$

The density of the mantle is in addition pressure dependent (β_m the coefficient of compressibility). The density profile for the lithospheric mantle is given by:

$$\rho_{\text{lm}}(z) = \rho_{\text{lmo}} \cdot (1 - \alpha_m \cdot T(z) + \beta_m \cdot P) \quad (3)$$

where ρ_{lmo} is the density of lithospheric mantle at room temperature. For the density profile in the asthenosphere, the density of the asthenosphere ρ_{ao} at room temperature is substituted in equation (3). To calculate the surface elevation, the lithospheric column is assumed to be in isostatic balance

with a column beneath the mid-ocean ridge whose elevation z_a represents the hydrostatic level of the asthenosphere. Following Le Pichon and Alvarez (1984), the hydrostatic level of the asthenosphere is assumed to be close to 3600 m. Therefore, the reference mid-ocean ridge column is formed of $z_a=3600$ m of water (density ρ_w) overlying $(f_1.z_1 + h - z_a)$ meters of asthenospheric mantle. When the surface of the deforming lithosphere is below sea level, it is assumed that one third of the basin ($h/3$) is filled with sediments.

4.3 Gravitational force

For simplicity flexural stresses induced by the elastic behavior of the lithosphere are not considered here. With depth (z) increasing downward from a sea level origin, the gravitational potential energy (Pe) per unit area of a lithospheric column is given by the integral of the vertical stress σ_{zz} from the bottom of the column at depth $f_1 z_1 + h$ to its top which is at an elevation h (when the column stands above sea level) or 0 (when it is below sea level):

$$Pe = \int_{f_1 z_1 + h}^{\text{surface}} \rho(z').g.z' dz' \quad (4)$$

where: $\rho(z')$ is the density profile, g is the gravitational acceleration, z' is the integration variable. Assuming local isostatic compensation, the gravitational force per unit length that the deformed lithosphere and the surrounding lithosphere apply to one another is given by the contrast in gravitational potential energy between the reference and deformed lithospheric column. It is the difference between the integrals of the vertical stress profile down to a compensation level L beneath the lithosphere.

$$F_g = \Delta Pe = \Delta \left[\int_L^S \left(\int_L^S \rho(z'').g.dz'' \right) dz \right] \quad (5)$$

S represents either the elevation of the reference lithosphere or that of the modified lithosphere, whichever is higher, L is the bottom of the reference lithosphere ($z_1 + h$) or that of the modified lithosphere ($f_1.z_1 + h$), whichever is the deepest.

4.4 Strength profile

In the rheological profile, frictional sliding describes failure mechanisms at low temperature and high strain rate (in the upper crust and the upper mantle, Sibson, 1974):

$$\sigma_1(z) - \sigma_3(z) = \beta \cdot \rho(z) \cdot g \cdot (z - h) \cdot (1 - \lambda) \quad (6)$$

with: g the gravitational acceleration, λ the ratio of fluid pore pressure to the normal stress, and β a parameter dependent on the type of faulting. At high temperatures the viscous deformation of the crust is modelled as power law creep:

$$\sigma_1(z) - \sigma_3(z) = \left(\frac{\dot{\epsilon}}{A_c}\right)^{1/n} \cdot \exp\left(\frac{Q_c}{n \cdot R \cdot T(z)}\right) \quad (7)$$

and in the mantle as power law creep and Dorn law creep depending on $(\sigma_1 - \sigma_3)$:

$$\sigma_1(z) - \sigma_3(z) = \left(\begin{array}{ll} \left(\frac{\dot{\epsilon}}{A_m}\right)^{1/n} \cdot \exp\left(\frac{Q_m}{n \cdot R \cdot T(z)}\right) & \text{for } (\sigma_1 - \sigma_3) < 200 \text{ MPa} \\ \sigma_d \cdot \left(1 - \sqrt{\frac{R \cdot T(z)}{Q_d} \cdot \ln\left(\frac{\dot{\epsilon}_d}{\dot{\epsilon}}\right)}\right) & \text{for } (\sigma_1 - \sigma_3) > 200 \text{ MPa} \end{array} \right) \quad (8)$$

Assuming a pure shear deformation and a constant strain rate with depth, the vertical integrated strength in extension (F_{edt}) and contraction (F_{edc}) of the lithosphere are respectively given by:

$$\left(\begin{array}{l} F_{edt} = \int_{z_l}^{z_d} \sigma_1(z) - \sigma_3(z) dz \quad \text{with } \beta = 0.75 \\ F_{edc} = \int_{z_l}^{z_d} \sigma_1(z) - \sigma_3(z) dz \quad \text{with } \beta = 3 \end{array} \right) \quad (9)$$

using the minimum of (6) and (7) for the crust and the minimum of (6), and (8) for the mantle.

4.5 Lithospheric geometry through time

The increase in crustal and whole lithospheric thicknesses over a small time interval (Δt) due to homogeneous pure shear are given by:

$$\dot{\epsilon}_t \cdot f_c \cdot z_c \cdot \Delta t \quad (10)$$

and

$$\dot{\epsilon}_t \cdot f_1 \cdot z_1 \cdot \Delta t \quad (11)$$

respectively. The thickening rate ($\dot{\epsilon}_t$) derives from balancing the tectonic force with the strength in contraction of the deforming lithosphere. Because of gravity-driven flow, the lithosphere tends also to thin. This thinning is given by:

$$\dot{\epsilon}_s \cdot f_1 \cdot z_1 \cdot \Delta t \quad (12)$$

When divergent gravitational collapse is accommodated by the passive displacement of the surrounding lithosphere, the spreading rate ($\dot{\epsilon}_s$) derives from balancing the gravitational force with the strength in extension of the deforming lithosphere. Alternatively when gravitational collapse is accommodated by the shortening of the lithosphere surrounding the orogenic domain, the spreading rate is buffered by either the strength in extension of the collapsing lithospheric column or the strength in contraction of the surrounding lithosphere.

5 Presentation of the results

In all of the experiments the reference lithosphere is shortened at a strain rate of 10^{-15} s^{-1} over a period of 30 Ma before to be unloaded. This shortening produces a 75 km thick crust and a 222 km thick lithosphere. In the first experiment, the thickened lithosphere is allowed to evolve under the action of erosion, gravitational force, and thermal relaxation. In the following experiments the thickness of the lithospheric mantle is instantaneously reduced to simulate the convective removal of the lower part of the lithosphere immediately after the end of convergence. The tectonic histories that unfold strongly depend on the amount of lithospheric mantle removed.

5.1 Stable Thermal Boundary Layer during convergence

The evolution of the vertical geometry of the deforming lithosphere is shown in Figure 3. At the end of convergence the gravitational force is compressive and relatively small ($1.70 \times 10^{12} \text{ Nm}^{-1}$) compared to the strength in contraction of the thickened lithosphere ($32.88 \times 10^{12} \text{ Nm}^{-1}$, strengths are given for a nominal strain rate of 10^{-15} s^{-1}). Through time, the strength of the lithosphere decreases but remains higher than that of the reference lithosphere. In contrast, the gravitational

force remains nearly constant. This suggests that over time the decay of the excess in gravitational potential energy stored in the crust is balanced by the decay through thermal relaxation of an equivalent deficit in gravitational potential energy stored in the lithospheric mantle. The lithosphere tends slowly to recover its initial geometry. 260 Ma after the end of convergence the continental crust and the lithosphere are still 45 km and 150km thick respectively, and the lithosphere is stronger than before deformation (Fig. 3). The tectonic evolution of the reference lithosphere can be summarised in two phases. In the first phase the lithosphere thickness increases during convergence. The second starts when the system is unloaded. During this phase the lithosphere slowly recovers its initial geometry over a few hundred of million years. At no stage during its evolution is the orogenic domain weaker than the reference lithosphere, and at no stage is the gravitational force stronger than the strength of the deformed lithosphere. This evolution is therefore characterised by an absence of significant collapse and the formation of a strong lithosphere that resists tectonic reactivation.

5.2 Post-convergence removal of the Thermal Boundary Layer

In this experiment the lower part of the lithosphere is removed at the end of convergence (to+30 Ma). Before convective thinning, the continental crust is then 75 km thick, the temperature at the Moho is 640°C, the elevation of the lithosphere is 4650 m, and its strength in extension has increased up to $24.5 \times 10^{12} \text{ Nm}^{-1}$. The gravitational force is low and compressive ($1.75 \times 10^{12} \text{ Nm}^{-1}$). Contrasting lithosphere geometries (Fig. 4) develop depending on the magnitude of the convective thinning. In the first example the entire lithosphere is thinned to 130 km, following the removal of the lower 92 km of the lithospheric mantle (Fig.4a1-2). As a result, the gravitational force switches from being slightly compressive to strongly extensive ($7.2 \times 10^{12} \text{ Nm}^{-1}$), whereas the strength in extension of the lithosphere is strongly reduced ($5 \times 10^{12} \text{ Nm}^{-1}$). The elevation increases to about 6600 m, and the temperature at the Moho increases to 780°C. Assuming that the surrounding undeformed lithosphere is passively displaced, the gravitational force is strong enough to produce thinning in the orogenic domain at a strain rate of 10^{-14} s^{-1} (Fig.4a3) which slowly decreases as divergent collapse proceeds. At to+33.6 Ma the lithosphere has recovered its initial thickness but the crust is 54 km thick. At this stage, divergent collapse is still very active with a strain rate of 10^{-15} s^{-1} . The thickness of the lithosphere decreases to 68 km by to+71.7 Ma, before increasing

again under the action of thermal relaxation. The crust continues to thin to 32 km, and by t_0+80 Ma the strain rate has dropped below 10^{-17} s^{-1} . A combination of erosion and thermal relaxation slowly brings the lithosphere towards its initial geometry over a time scale of a few hundred million years. This experiment is characterised by a vigorous phase of divergent collapse. The surface elevation remains above sea level although the crust becomes a bit thinner than its initial thickness. After a few hundred of Ma, the entire lithosphere will probably end up being a bit thicker than it was initially, because of a slightly thinner radiogenic crustal layer. A similar history unfolds when the lower 95km of the lithospheric mantle is removed (Fig. 4b). However, the collapse stage is longer than in the previous experiment, and at the end of it (t_0+112 Ma), the crust and the entire lithosphere are 19km and 33 km thick respectively, significantly thinner and therefore weaker than the reference lithosphere. The surface elevation of the lithosphere has dropped below sea level by t_0+65 Ma. Following thermal relaxation and sedimentation, the thickness of both the lithospheric mantle and the crust increases slowly. At t_0+200 Ma the whole lithosphere and the crust are 52 km and 22 km thick respectively. When the lower 97 km of the lithosphere is removed (Fig. 4c), divergent collapse results in active continental rifting following the development of a necking instability at around t_0+42 Ma (Fig. 4c2-3).

6 Discussion and conclusion

The simple 1D numerical experiments presented in this paper suggests that finite lithospheric thinning and active rifting can be the result of convective thinning of the thermal boundary layer following lithospheric thickening. The fact that divergent collapse results in a lithosphere thinner than the reference lithosphere is not surprising. The gravitational force that promotes thinning following convective thinning has its origin in the large excess in gravitational potential energy stored in the thickened crust (Fig. 5). In contrast, the gravitational potential energy stored in the lithospheric mantle is quite small and promotes compression. As collapse and homogeneous thinning proceed both the crust and the mantle becomes thinner. The excess in gravitational potential energy stored in the crust decreases, whereas thinning of the lithospheric mantle produces an increasing excess of gravitational potential energy (Fig. 5) that eventually promotes further thin-

ning. The experiments presented above show that, when enough lithospheric mantle is removed, this thinning leads towards a necking instability and the development of an active rift. The volume of lithospheric mantle that has to be removed to produce active rifting is not unrealistic. A study from Houseman and Molnar (1995) has shown that, for dry olivine, the section of the lithosphere hotter than 910-950°C is likely to be dragged into the convective mantle. For wet olivine, it is the section hotter than 750°C that can be instable. In the numerical experiments presented above, active rifting occurs when the section of the lithosphere hotter than 800°C is removed. There are many examples that suggest that divergent collapse has resulted in net crustal and lithospheric thinning. This is possibly the case in the Basin and Range Province where the crust, following Tertiary divergent collapse, is now 20-25 km thick and still under tensile stresses. The Carpathian Basin is another example of a low standing thin crust whose thinning has been related to post-thickening collapse. The Alboran Sea and the Aegean Sea, both the locus of very active divergent collapse during the Neogene, illustrate the case where the surface of the thinned lithosphere has dropped below sea level. In all these examples the thinned region, some still under tensile stresses, are surrounded by regions of compressive stresses that may have inhibited, so far, active rifting. It is possible that one of the most obvious manifestation of post-thickening active rifting occurs in the development of back-arc basins involving the opening of an oceanic domain that detaches a piece of continental lithosphere from a thickened continental passive margin. Indeed, any mechanism that thins the sub-continental lithospheric mantle above a subduction zone will produce tensile stresses that may promote (i) failure of the overriding lithosphere, (ii) divergent collapse, (iii) active rifting, and (iv) opening of a back-arc basin. Figure 6 sketches the situation whereby the thermal boundary layer of the overriding plate is dragged into the convective mantle by the descending oceanic slab. As long as the subduction zone acts as a free boundary, the broken lithosphere segment will move counter to the subduction plate as the back-arc basin develops. Back-arc dynamics has been successfully produced in physical models (Shemenda, 1993). This modelling shows that a zone of weakness in the overriding plate is necessary for back-arc extension to develop. Collapse following thickening of the overriding plate may produce this zone of weakness.

7 Acknowledgements

This paper has benefited from helpful and constructive reviews from O. Vanderhaeghe and P. Ryan. Many thanks to G. Houseman, S. Costa, M. Jessell, and W. Schellart, for countless conversations and arguments. Thanks to S. Van Huet for having improved the english, and J. Miller for editing the text. This work was supported by ARC Large Grant No: A10017138.

8 References

Ahnert, F., 1970. Functional relationships between denudation, relief, and uplift in large mid-latitude drainage basins. *American Journal of Science*, 268, 243-263.

Artyushkov, E.V., 1973. Stresses in the lithosphere caused by crustal thickness inhomogeneities. *Journal of Geophysical Research*, 78, 7675-7708.

Bott, M.H.P., 1993. Modelling the plate-driving mechanism. *Journal of Geological Society, London*, 150, 941-951.

Buck, R., 1991. Modes of continental lithospheric extension. *Journal of Geophysical Research*, 96 (20), 161-20, 178.

Clark, S.P., and E. Jaeger, 1969. Denudation rates in the Alps from geochronological and heat flow data. *American Journal of Science*, 267, 1143-1160.

Cochran, J.R., 1983. Effect of finite rifting times on the development of sedimentary basins. *Earth and Planetary Science Letters*, 66, 289-302.

Coney, P.J., and T.A., Harms, 1984. Cordilleran metamorphic core complexes: Cenozoic extensional relics of Mesozoic compression. *Geology*, 12, 550-554.

Costa, S., and Rey, P., 1995. Lower crustal rejuvenation and growth during post-thickening collapse: Insights from a crustal cross section through a Variscan metamorphic core complex. *Geology*, 23, pp. 905-908.

Coward, M. 1994. Inversion Tectonics. In: P. L. Hancock (Ed.), *Continental Deformation*, Pergamon Press, Oxford, 289-304.

Dalmayrac, B, and Molnar, P., 1981. Parallel thrust and normal faulting in Peru and constraints on the state of stress. *Earth and Planetary Science Letters*, 55, pp. 473-481. Dewey, J.F., 1988. Extensional collapse of orogens. *Tectonics* 7, 1123-1139.

Dewey, J.F., Ryan, P.D., Andersen, T.B., 1993. Orogenic uplift and collapse, crustal thickness, fabrics and metamorphic phase changes: the role of eclogites. In: H.M. Prichard, T. Alabaster, N.B.W. Harris and C.R. Neary (Eds.), *Magmatic processes and plate tectonics*, *Geol. Soc. London Spec. Publ.*, 76, 325-343.

England, P.C., McKenzie, D.P., 1982. A thin viscous sheet model for continental deformation.

Geophys. J. R. Astron. Soc., 70, 295-321.

England, P.C., McKenzie, D.P., 1983. Correction to: A thin viscous sheet model for continental deformation. *Geophys. J. R. Astron. Soc.*, 73, 523-532.

England, P.C., Houseman, G.A., 1988. The mechanics of the Tibetan plateau. *Phil. Trans. R. Soc. London*, 326, 301-320.

England, P.C., Houseman, G.A., 1989. Extension during continental convergence, with application to the Tibetan Plateau. *J. Geophys. Res.* 94, 17561-17579.

England, P.C., and S.W., Richardson, 1977. The influence of erosion upon mineral facies of rocks from different metamorphic environments. *J. Geol. Soc. London*, 134, pp. 201-213.

Fleitout, L., Froidevaux, C., 1982. Tectonics and topography for a lithosphere containing density heterogeneities. *Tectonics*, 1, 21-56.

Govers, R., and Wortel, M.J.R., 1995. Extension of stable continental lithosphere and the initiation of lithospheric scale faults. *Tectonics*, 14, 4, 1041-1055.

Houseman, G. A., D. P., McKenzie, and P. Molnar, 1981. Convective instability of a thickened boundary layer and its relevance for the thermal evolution of continental convergent belts. *J. Geophys. Res.*, 86, pp. 6115-6132.

Houseman, G. A., England, P.C., 1986. A dynamic model of lithosphere extension and sedimentary basin formation. *J. Geophys. Res.*, 91, 719-729.

Houseman, G. A., and Molnar, P.C., 1997. Gravitational (Rayleigh-Taylor) instability of a layer with non-linear viscosity and convective thinning of continental lithosphere. *Geophys. J. Int.*, 128, 125-150.

Jarvis, G.T., McKenzie, D.P., 1980. Sedimentary basin formation with finite extension rates. *Earth Planet. Sci. Lett.*, 48, p.42-52.

Le Pichon, X., 1983. Land-locked oceanic basins and continental collision: The eastern mediterranean as a case example. In: K.J. Hsu (Ed.), *Mountain Building Processes*, Academic Press, New York, pp. 201-211.

Le Pichon, X., and F. Alvarez, 1984. From stretching to subduction in back-arc regions: Dynamic considerations. *Tectonophysics*, 102, pp. 343-357.

Mareschal, J.C., 1994. Thermal regime and post-orogenic extension in collision belts. *Tectono-*

physics, 238, pp. 471-484.

McKenzie, D.P., 1978. Some remarks on the development of sedimentary basins. *Earth Planet. Sci. Lett.*, 40, p.25-32.

Mercier, L, Lardeaux, J.M., and P. Davy, 1991. On the tectonic significance of retrograde P-T-t paths in eclogites of the French Massif Central. *Tectonics*, v.10, n1, pp. 131-140.

Molnar, P., Tapponnier, P., 1975. Cenozoic tectonics of Asia: Effects of a continental collision. *Science*, 189, 419-426.

Molnar, P., Tapponnier, P., 1978. Active tectonics of Tibet. *J. Geophys. Res.*, 83, 5361-5375.

Molnar, P. and Chen, W.P., 1982. Seismicity and mountain building. , in Hsu, K, J, ed., *Mountain building processes. New York, Academic Press*, pp. 41-57.

Molnar, P. and Chen, W.P., 1983. Focal depths and fault plane solutions earthquakes under the Tibetan plateau. *J. Geophys. Res.* 88, 1180-1196.

Molnar, P., and Lyon-Caen, H., 1988. Some simple physical aspects of the support, structure and evolution of mountain belts. *Geol. Soc. Am. Spec.*, Pap. 218, 179-207.

Pinet, P. and Souriau, M., 1988. Continental erosion and large-scale relief. *Tectonics*, v.7, 3, pp. 563-582.

Platt, J.P., and P.C., England, 1993. Convective removal of the lithosphere beneath mountain belt: thermal and mechanical consequences. *Am. J. Sci.*, v.294, 307-336.

Ranalli, G., 1992. Average lithospheric stresses induced by thickness change: A linear approximation. *Phys. Earth Planet. Int.*, 69, 263-269.

Ranalli, G., 1995. *Rheology of the Earth. Chapman & Hall, London, UK*, 413 pp.

Rey, 1993. Seismic and tectono-metamorphic characters of the lower continental crust in Phanerozoic areas: A consequence of post-thickening extension. *Tectonics*, 12, 2, pp. 580-590.

Rey, P., Vanderheaghe, O., and Teyssier, C., 2001. Gravitational collapse of continental crust: Definition, regimes, and modes. *Tectonophysics*, in press.

Richter, F.M., McKenzie, D.P., 1978. Simple plate models of mantle convection. *J. Geophys.*, 44, 441.

Royden, L., and Keen, C.E., 1980. Rifting process and thermal evolution of the continental margin of eastern Canada determined from subsidence curves. *Earth Planet. Sci. Lett.*, 51, p.343-

361.

Ruxton, B.P., and I. McDougall, 1967. Denudation rates in northeast Papua from potassium-argon dating of lavas. *Am. J. Sci.*, 265, pp. 545-561.

Sandiford, M., and Powell, R., 1990. Some isostatic and thermal consequences of the vertical strain geometry in convergent orogens. *Earth Planet. Sci. Lett.*, 98, 154-165.

Sandiford, M., and Powell, R., 1991. Some remarks on high-temperature low-pressure metamorphism in convergent orogens. *J. Meta. Geol.*, 9, 333-340.

Sandiford, M., Foden, J., Zhou, and S., Turner, S., 1992. Granite genesis and mechanics of convergent orogenic belts with application to the southern Adelaide fold belt. *Trans. R. Soc. Edinburgh: Earth Sciences*, 83, 83-93.

Shemenda, A.I., 1993. Subduction of the lithosphere and back-arc dynamics: Insights from physical modeling. *Journal of Geophys. Res.*, 98, pp. 16167-16185.

Sibson, R.H., 1974. Frictional constraints on thrust, wrench and normal faults, *Nature*, 249, 542-544.

Sonder, L.J., England, P.C., 1986. Vertical averages of rheology of continental lithosphere: relation to thin sheet parameters. *Earth Planet. Sci. Lett.*, v.77, p.81-90.

Sonder, L., England, P.C., Wernicke, B.P., Christiansen, R.L., 1987. A physical model for Cenozoic extension of western North America. In: M.P. Coward, J.F. Dewey and P.L. Hancock (Eds.), *Continental Extensional Tectonics*, *Geol. Soc. London Spec. Publ.*, 28, 187-201.

Sun, J., Murrell, A.F., 1989. On the growth and collapse of wide orogenic belts. *Geophys. J. Int.*, 118, 255-268.

Turcotte, D. L., and S. H., Emerman, 1983. Mechanisms of active and passive rifting. *Tectonophysics*, 94, pp. 39-50.

Zhou, S., Sandiford, M., 1992. On the stability of isostatically compensated mountain belts. *J. Geophys. Res.*, 97, 14207-14221.

Table 1: List of Parameter values

Gravity g , $m.s^{-2}$	9.81
Crust thermal expansion coefficient α_c , $10^{-5} K^{-1}$	3.5
Mantle thermal expansion coefficient $\alpha_m = a_0 + a_1.T + a_2.T^2$, K^{-1}	$a_0 = 2.697.10^{-3}$ $a_1 = 1.0192.10^{-8}$ $a_2 = -0.1282$
Mantle bulk modulus β_m , MPa	130
Lithosphere thermal diffusivity κ , $\mu m^2 s^{-1}$	0.97
Lithosphere thermal conductivity, $W m^{-1} K^{-1}$	3.1
Crust volumetric heat production, $\mu W m^{-3}$	0.80
Mantle volumetric heat production, $\mu W m^{-3}$	0
Surface temperature T_0 , K	273
Temperature at the base of the lithosphere T_l , K	1603
Heat Flow at the base of the lithosphere Q_0 , $mW m^{-2}$	34.9
Crustal thickness z_c , km	35
Lithosphere thickness z_l , km	104
Neutral buoyant level of asthenosphere z_a , km	-3.6
Lithospheric mantle density ($T=T_0$) ρ_{lmo} , $kg m^{-3}$	3370
Asthenospheric mantle density ($T=T_0$) ρ_{ao} , $kg m^{-3}$	3390
Crust mass density @ $z=h$, ρ_a , $kg m^{-3}$	2670
Crust mass density @ $z=z_c$, ρ_b , $kg m^{-3}$	2950
Water mass density, ρ_w , $kg m^{-3}$	1030
Ratio pore pressure to overburden stress λ ,	0.36
Universal gas constant R , $J.mol^{-1}.K^{-1}$	8.3144
Crust power law sensitivity n_c ,	3
Crust power law activation enthalpy Q_c , $kJ mol^{-1}$	190
Crust power law pre-exponent A_c , $MPa^{-3} s^{-1}$	5.10^{-6}
Mantle power law sensitivity n_m ,	3
Mantle power law activation enthalpy Q_m , $kJ mol^{-1}$	520
Mantle power law pre-exponent A_m , $MPa^{-3}.s^{-1}$	7.10^4
Mantle Dorn plasticity law activation enthalpy Q_d , $kJ mol^{-1}$	540
Mantle Dorn plasticity law stress treshold σ_d , MPa	8500
Mantle Dorn plasticity law strain rate ϵ_d , s^{-1}	$3.05. 10^{11}$

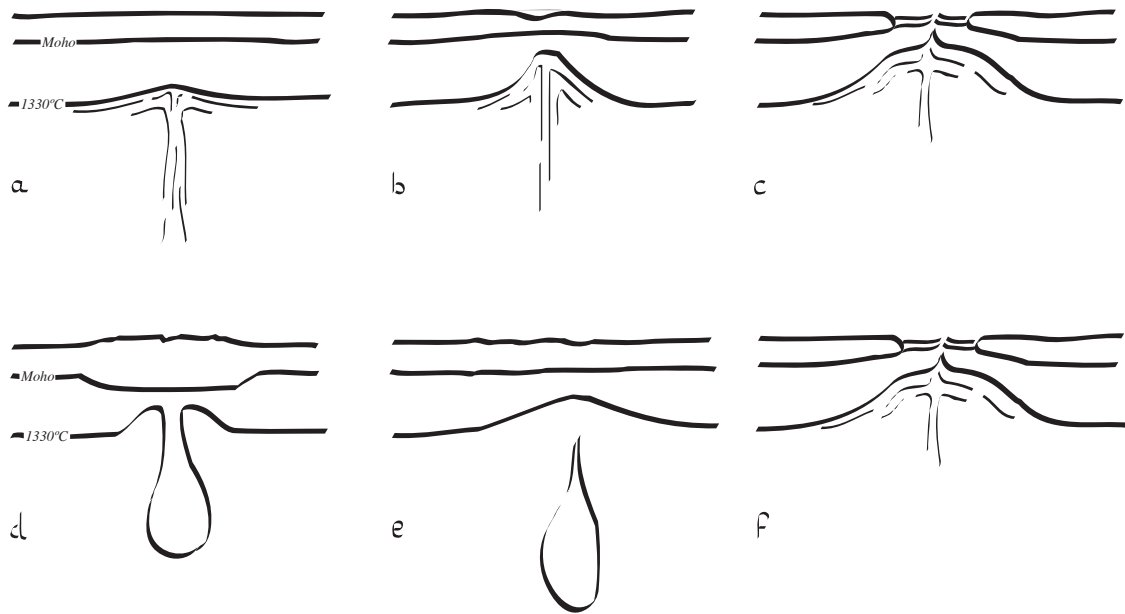


Figure 1: Thinning of the lithospheric mantle related to a thermal plume (a, b), or following the convective thinning of the thermal boundary layer of the lithosphere (d, e), may result in active continental rifting (c, f).

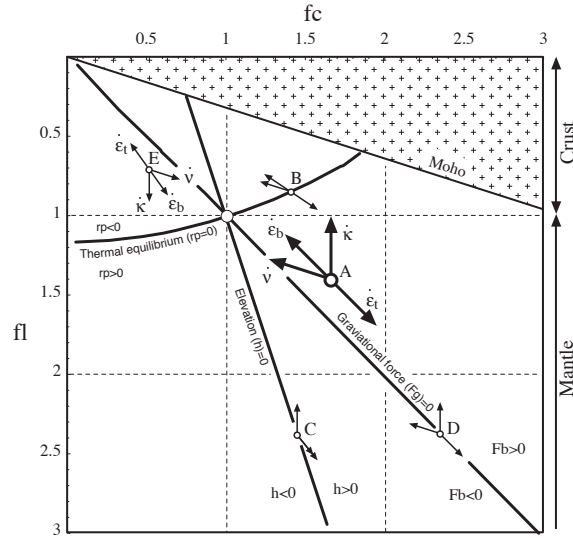


Figure 2: Four elementary processes may affect the vertical geometry of the lithosphere (i.e. the thickness of the crust and that of the lithospheric mantle). These processes can be represented as vectors in the f_c - f_l plane. For example the lithosphere A is subjected to the action of erosion (?), tectonic thickening (ϵ_t), gravity-driven flow (ϵ_b), and thermal relaxation (κ). The path followed by the lithosphere A in the f_c - f_l plane depends on the magnitude of the four vectors and their respective orientation. The length of each vector represents its rate. Lithosphere E is also subjected to the action of the four processes but all the vectors have a direction opposite to lithosphere A. Indeed, the gravity-driven flow is divergent and tends to thin the lithosphere when the gravitational force is positive (the deformed lithosphere has an excess of gravitational potential energy). However, when the gravitational force is negative the gravity-driven flow has an opposite effect. When the elevation is positive erosion tends to reduce the thickness of the crust. In contrast, when elevation is negative, sedimentation tends to increase the thickness of the crust. Thermal relaxation may induce the thickening or the thinning of the lithospheric mantle depending of the sign of the thermal potential (r_p , Sandiford and Powell, 1991). Lithosphere B, C, and D represent cases where only three processes are active.

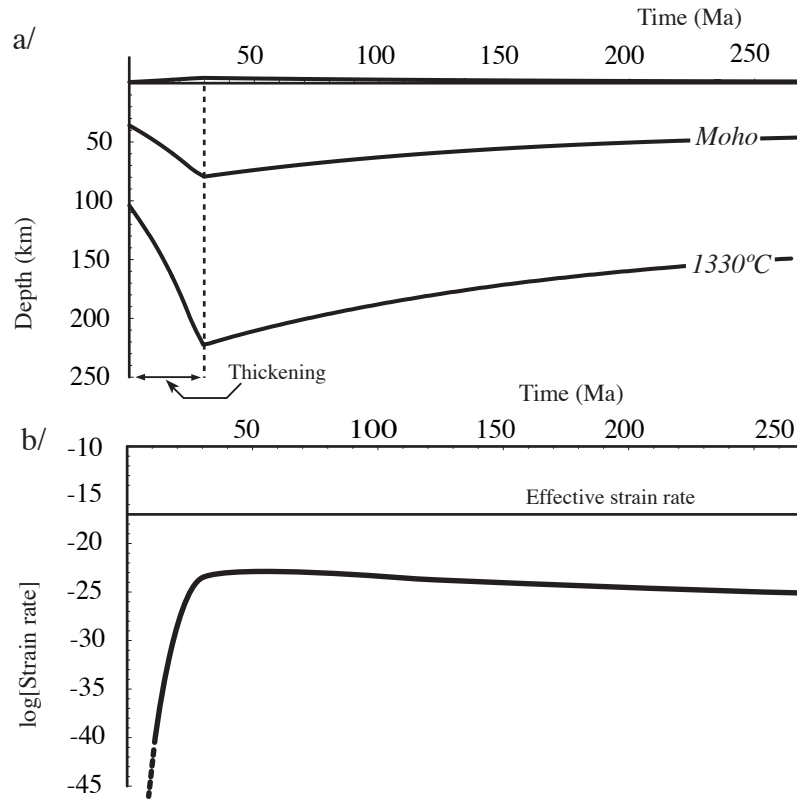


Figure 3: a/ Evolution of the geometry of the lithosphere assuming a homogeneous tectonic thickening. Thickening last for 30 Ma, the thermal boundary layer is stable. Erosion and thermal relaxation slowly bring back the lithosphere towards its original geometry over a time scale of a few hundreds of Ma. b/ Evolution of the spreading rate. At no time is the spreading rate higher than the effective strain rate (10^{-17} s^{-1}). Divergent collapse is therefore not significant.

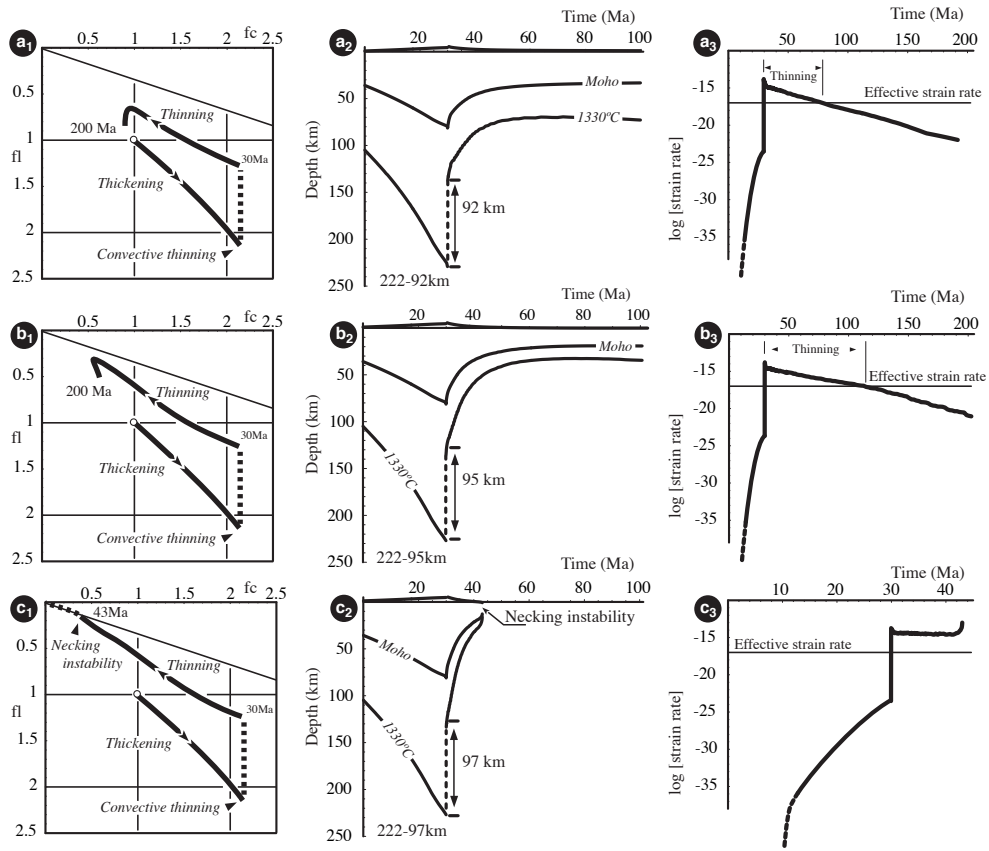


Figure 4: Evolution of the geometry of the lithosphere following homogeneous tectonic thickening and convective thinning of the thermal boundary layer. Convergence lasts for 30 Ma, and convective thinning occurs immediately after convergence. Collapse is assumed to be accommodated by the passive displacement of the surrounding lithosphere. Three situations are considered whereby the bottom 92, 95, and 97 km are removed from the lithosphere (rows from top to bottom respectively). The evolution of the lithospheric geometry is shown in the f_c - f_l plane (diagrams in the left column), as well as in a diagram showing the depth versus time of the main density interfaces (diagrams in the central column). Diagrams in the right column show that for each experiment significant gravity-driven flow occurs following convective thinning of the lithospheric mantle (i.e. spreading rate is higher than 10^{-17} s^{-1}).

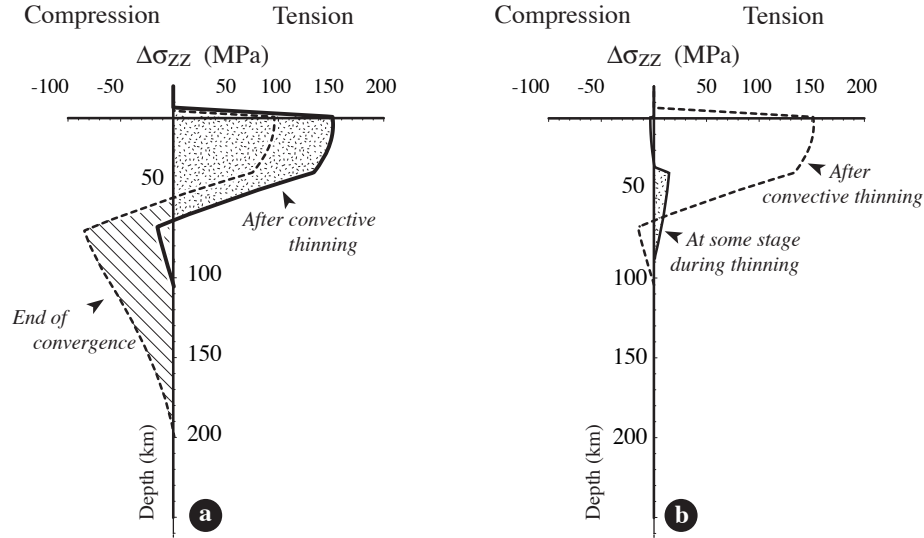


Figure 5: The contrast in gravitational potential energy between a deformed lithospheric column and its surroundings is given by the integral of the difference in lithostatic pressure ($\Delta\sigma_{zz}$) along a deformed lithospheric column and along a column of the surrounding lithosphere. (a) At the end of thickening (dashed line), an excess in gravitational energy (promoting extension) is stored in the upper part of the lithosphere (mostly the crust), whereas there is a deficit in potential energy (which promotes compression) in the lower part of the lithosphere. After convective thinning of the thermal boundary layer (thick solid line), most of the deficit in potential energy is removed whereas the excess in potential energy increases significantly. The whole lithosphere is therefore under strong horizontal tensile stresses which leads to divergent collapse and thinning. (b) As collapse proceeds, the excess of gravitational potential energy is reduced and at one stage the crust starts to accumulate a deficit in gravitational potential energy (thin solid line). In the meantime the thinning mantle starts to store excess in gravitational potential energy. It is this excess that promotes self-enhanced extension that may lead to active continental rifting.

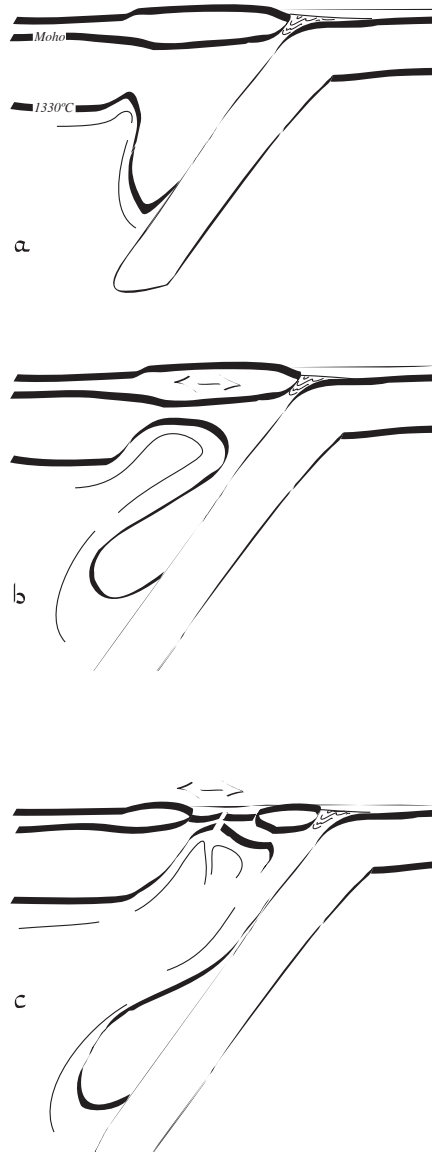


Figure 6: Back-arc extension as an example of post-convective thinning active continental rifting. This figure illustrates how the thinning of the lithospheric mantle underneath a thickened crust may induce active continental rifting, provided that the subduction zone acts as a free boundary. The force driving active continental rifting is the gravitational force related to the differential thinning of the lithospheric mantle.